# Use of Magnetotactic Bacteria as an MRI Contrast Agent for In Vivo Tracking of Adoptively Transferred Immune Cells

**Andrea Nuschke**
Dalhousie University
**Caitrin Sobey-Skelton**
Dalhousie University
**Bassel Dawod**
Dalhousie University
**Brianna Kelly**
Dalhousie University
**Marie-Laurence Tremblay**
Nova Scotia Health Authority
**Christa Davis**
Izaak Walton Killam Hospital for Children: IWK Health Centre
**James A. Rioux**
Dalhousie University
**Kimberly Brewer** ( brewerk@dal.ca )
Dalhousie University https://orcid.org/0000-0001-7973-0126

**Research Article**

**Keywords:** Magnetoendosymbionts (MEs), cell tracking, magnetic resonance imaging (MRI), cytotoxic T lymphocytes (CTLs), myeloid lineage cells (MLCs), dendritic cells (DCs), myeloid-derived suppressor cells (MDSCs)

**Posted Date:** May 19th, 2023

**DOI:** https://doi.org/10.21203/rs.3.rs-2939089/v1

## Abstract

# Purpose

*In vivo* immune cell tracking using MRI is a valuable tool for studying the mechanisms underlying successful cancer therapies. Current cell labeling methods using superparamagnetic iron oxide (SPIO) lack the specificity and persistence needed to track the fate and location of transplanted cells long-term. *Magnetospirillium magneticum* is a commercially available, iron-producing bacterium that can be taken up by, and live harmoniously within, mammalian cells as magneto-endosymbionts (MEs). MEs have shown promise as labeling agents for *in vivo* stem and cancer cell tracking but have yet to be evaluated in immune cells. This pilot study examined ME labeling in myeloid-derived suppressor cells (MDSCs), cytotoxic T lymphocytes (CTLs) and dendritic cells (DCs) and its effects on cell purity, function and MRI contrast.

# Procedures:

MDSCs, CTLs and DCs were incubated with MEs at various ME labelling ratios (MLR) and various biological metrics and iron uptake were assessed. For *in vivo* imaging, MDSCs were labeled overnight with either MEs or SPIO (Molday ION Rhodamine B) and injected into C3 tumor-bearing mice via tail vein injection 24 days post-implant and scanned daily with MRI for one week to assess cellular quantification.

# Results

Following incubations MDSCs contained 0.62 and 2.22 pg Fe/ cell. CTLs achieved Fe loading of < 0.5 pg/ cell and DCs achieved Fe loading of ~ 1.4pg/cell. The suppressive functionality of MDSCs at 1000MLR was not affected by ME labeling but was affected at 2000MLR. Markers of CTL dysfunction were not markedly affected by ME labeling, nor were DC markers. *In vivo* data demonstrated that the MDSCs labeled with MEs generated sufficient contrast to be detectable using TurboSPI, similar to SPIO-labeled cells.

# Conclusions

Cells can be labeled with pre-clinically relevant amounts of MEs without compromising cell viability. Care must be taken at higher concentrations of MEs, which may affect the functional activity and/or morphology of some cell types. Immune cells with minimal phagocytic behaviour have much lower iron content per cells after incubation with MEs vs SPIO; however, MEs can successfully be used as a contrast agent for phagocytic immune cells.


## INTRODUCTION

With the rapid advancement of personalized therapies in cancer, including adoptive cell transfer (ACT), peptide vaccines, and dendritic cell-based vaccines, the need to track therapy biodistribution and cell fate *in vivo* has grown considerably. For example, ACT of autologous lymphocytes (e.g. tumour-infiltrating lymphocytes, or TILs; engineered T-cell receptor, or TCRs; and chimeric antigen receptor T-lymphocytes, or CAR-T cells) has shown promise in the treatment of selected metastatic cancers[1,2]. However, a fundamental requirement for therapeutic success is that cells migrate effectively to, and remain in, the correct target organ or tissue[3].

One approach to assess the distribution of adoptively transferred cells in the body is to label cells with superparamagnetic iron oxide (SPIO) nanoparticles *ex vivo* and then track their migration with magnetic resonance imaging (MRI) following injection. SPIO-labelled cell tracking with MRI is a powerful technique that can provide 3D resolution of therapy location in tandem with rich anatomical details of disease progression, such as tumour size, shape, and metastases. The applications of SPIO MRI contrast agents are broad – through *in vivo* tracking of tumours[4–7], therapies[8], immune cells[9–13] and vaccines[14], as well as other uses, they can serve as valuable tools in the early detection of disease and the study of disease mechanisms and progression.

*Ex vivo* cell labelling is achieved by incubating cells for a short time (often 24 hours or less) in culture media containing SPIO particles. Cells internalize the particles, achieving intracellular iron concentrations in the nanogram (ng) to picogram (pg) range, depending on cell type and duration of incubation, without significant detriment to cell function[15–17]. With higher levels of intracellular iron, MRI cell-tracking has even achieved single-cell resolution *in vivo*[18]. However, the long-term fidelity of the SPIO signal *in vivo* is limited by the potential for signal dilution in dividing cell types and the generation of false positive signal through uptake of SPIO by resident macrophages following the release of the particles from dead cells[19].

Recently, magnetotactic bacteria have drawn interest for their ability to synthesize highly pure, membrane-enveloped chains of magnetite ($Fe_3O_4$) crystals – particles that are often referred to as magnetosomes – that demonstrate strong effects on both $T_1$ and $T_2$ relaxation time[20,21]. Through a process called endosymbiosis, non-pathogenic magnetotactic bacteria can be taken up by, and live harmoniously within, host mammalian cells, thereby becoming magneto-endosymbionts (MEs). Importantly, when the host cell dies the magnetite chains should rapidly lose their structure, reducing the likelihood of false positives[22] and demonstrating the potential value of MEs as a live-cell-specific cell tracking agent in longitudinal studies.

For magnetotactic bacteria and/or their magnetosomes to be used to track migrating cells *in vivo* effectively, they must be sufficiently internalized within the cells of interest and persist long enough to allow subsequent imaging. A select number of studies have examined the cell-tracking capabilities of MEs in various cell types following the internalization of either the isolated magnetosomes or entire bacteria. Schwarz and colleagues[23] demonstrated that the intracellular iron load following uptake of isolated magnetosome particles into mouse Flt3 + stem cells and dendritic cells from bone marrow

(approximately 30 pg in DCs and 17 pg in Flt3 + stem cells) was comparable to loading achieved with a synthetic particle label, and cell viability was not affected. Iron loading was sufficient to detect i*n vivo* migration of DCs towards draining lymph nodes in a mouse with MRI following intradermal transplantation into the hind leg. Human cervix epithelial (HeLa) cells have been shown to retain isolated magnetosomes beyond 120 hours following internalization with little to no degradation of the magnetic particles[24]. These studies demonstrate that isolated magnetosomes can provide strong enough MR signals for cell tracking studies for a duration of at least 5 days following labelling. Loading of cells with magnetosomes appears to have little effect on cell viability and function, even with extended incubation times and intracellular iron concentrations that exceed those achieved with synthetic magnetic particles. Indeed, isolated magnetosomes seem to be even better tolerated than synthetic magnetic particles by a variety of cell lines[23–25].

The use of MEs, i.e. internalization of the whole bacterium rather than the isolated magnetosome, has also shown promise as an MR contrast agent in a handful of studies. Mahmoudi and colleagues[22] evaluated ME labelling in human induced pluripotent stem cell (iPSC)-derived cardiomyocytes (iCMs) *in vitro* and *in vivo* following injection into the mouse myocardium. Labelled iCMs demonstrated higher viability (93%) than unlabelled cells (88%) and markers of healthy myocyte function were preserved. Upon injection into the myocardium, the ME signal could be readily detected with MRI and showed good correlation to a concurrent viability-dependent bioluminescent signal, suggesting the strong potential of MEs as a live-cell specific agent. Notably, when compared to SPIO (Molday ION) labelling of iCMs in the same model, the Molday signal persisted well after the extinction of the bioluminescent signal, suggesting the likelihood of false-positive signal detection over time when using synthetic magnetic particles. In another study[5], a direct comparison between SPIO Molday ION Rhodamine B and MEs as contrast agents for *in vitro* and preclinical *in vivo* detection of human breast adenocarcinoma cells revealed that even with conservative measurements, transverse relaxivity ($R_2$; equivalent to the inverse of $T_2$) values of MEs were significantly higher than those of Molday particles, demonstrating the innate strength of MEs as potential MRI contrast agents. Taken together, these studies demonstrate the potential value of MEs as reliable live-cell-specific contrast agents for cell tracking with MRI.

As mentioned above, whole magnetotactic bacteria as intracellular contrast agents may allow replication of the bacteria, potentially limiting attenuation of the signal over time, and passing down of signal to daughter cells following meiosis. To this point, Lee and colleagues[26] evaluated the intracellular fate of MEs in human breast adenocarcinoma cells and found that, while ME digestion proceeds naturally by the lysosomal pathway, MEs coated with listeriolysin were able to temporarily evade degradation. While a full understanding of the fate of intracellular MEs over time has yet to be achieved, manipulation of MEs, either chemically or genetically, may allow MEs to persist for longer periods of time within living cells, increasing their value in longitudinal imaging studies[26]. As with isolated magnetosomes, internalization of MEs did not appear to affect cell viability or function in mice receiving transplants of ME-labelled cells[5,22,26]. Furthermore, evaluation of blood markers and histopathology following direct intravenous (i.v.), intramuscular (i.m.) and intrathecal (i.t.) injection of MEs in rats suggests that MEs are most likely

not immunogenic. This evidence of biocompatibility, at both the cellular and organismal level, along with the strong MR signal generated by ME-labelled cells *in vivo*, suggests MEs are a candidate as a contrast agent for preclinical cell-tracking with MRI, with translatability to the clinical imaging milieu.

The success of studies using MEs in cancer cells and cardiomyocytes is encouraging; however, more work is required to assess the compatibility, reliability, and strength of MEs as contrast agents for studies of immune cell tracking. Although Schwarz and colleagues[23] demonstrated that isolated magnetosomes produced good MR contrast and were well tolerated in DCs, there are currently no examples of ME labelling with *in vivo* cell tracking in immune cells. In the present study, we compared MEs to SPIO as a cell-tracking contrast agent for three immune cell types, isolated from mice, that are known to play critical roles in anti-tumour immunity: cytotoxic T lymphocytes (CTLs), dendritic cells (DCs), and myeloid-derived suppressor cells (MDSCs). Iron assays were used to measure the uptake of MEs and intracellular iron in each cell type. Flow cytometry, immunohistochemistry (IHC), and live-cell assays were used to assess cell phenotype and functionality before and after ME labelling. The strength of MRI contrast of labelled cells was assessed *in vitro* using traditional gradient-echo and balanced steady-state free precession pulse sequences. Finally, we used MRI, flow cytometry, and IHC to compare the migration and persistence of i.v.-injected homologous MDSCs labelled with either a traditional SPIO-Rhodamine B label or MEs in a murine model of cervical cancer.

# MATERIALS & METHODS

## General Methods & Materials

### Animals

Female C57BL/6-Tg(UbC-GFP)30Scha/J mice (n = 6) obtained from Jackson Laboratories (Bar Harbour, MN, US) were used as donor mice for cell isolations. Female C57BL/6 mice (4–6 weeks old) were obtained from Charles River Laboratory (St. Constant, QC, Canada) and were bred in-house. For *in vivo* experiments, 6 GFP + mice were used as donor mice and n = 13 C57BL/6 mice were used as recipient mice for labelled MDSC injections and subsequent imaging. All mice had access to food and water ad libitum and were housed under filter-top conditions. All animal experiments were carried out in accordance with protocols approved by the University Committee on Laboratory Animals at Dalhousie University, Halifax, N.S., Canada.

### C3 Culture and Implantation

The murine cervical cancer C3 cell line obtained from Dr. Martin Kast (University of Southern California) was cryopreserved in fetal bovine serum (FBS, VWR/Avantor, Radnor, PA, US) + 10% dimethylsulfoxide (DMSO, VWR/Avantor) in liquid nitrogen[27], was maintained in complete DMEM (cDMEM), which was DMEM (Corning, Tewksbury, MA, US) supplemented with 10% FBessence (VWR/Avantor), 5mM L-glutamine (VWR/Avantor), 100 U/mL Penicillin/streptomycin (Gibco, Billings, MT, US), 55 μM of b-

mercaptoethanol (Gibco), and 10 mM HEPES (MilliporeSigma, Burlington, MA, USA). C3 cells were grown in the incubator at 37$^{o}$C and 5% $CO_2$ and harvested at 70% confluency after at least one passage. For the *in vivo* study, mice were implanted in the left flank via subcutaneous (s.c.) injection with 5 x $10^5$ C3 cells suspended in 200 µL of Hank's Balanced Salt Solution (HBSS, Corning) with 20 mM HEPES.

# Tumour Monitoring

Tumours were measured with calipers weekly beginning 6 days post-C3 implant. The formula [(shortest measurement)$^2$ x (longest measurement) /2] was used to calculate tumour volume. Once tumours reached 1000 mm$^3$, measurements were performed twice weekly until the end of the study. Mice were terminated if tumour volumes exceeded 2000mm$^3$.

# Cell Isolations

Mice used for cell isolations were euthanized by $CO_2$ inhalation at 20 days following C3 implantation.

# 1) CTLs

Inguinal, axillary, brachial, mesenteric, and submandibular lymph nodes (LNs) were excised and T-cells isolated as previously described (Tremblay et al., 2017). Briefly, CD8 + CTLs were enriched by panning and cultured at a density of 1 x $10^6$ cells/mL in complete RPMI (cRPMI) media supplemented with CD28 (1 µg/mL; clone 37.51, Tonbo Biosciences, San Diego, CA, USA), gentamycin (5 µg/mL, Gibco), IL-2 (100 U/mL, Peprotech, Rocky Hill NJ, UA), IL-12 (1 ng/mL, MilliporeSigma) in culture dishes that had been pre-coated overnight with 1 µg/mL CD3 (clone 145-2C11, Tonbo Biosciences) in phosphate buffered saline (PBS, 1X concentration; Corning). cRPMI media was a solution of RPMI 1640 (MilliporeSigma) with 10% FBessence, 100 U/mL of Penicillin/Streptomycin, 55 µM of b-mercaptoethanol, and 10 mM HEPES. Cells were maintained with fresh cRPMI media supplemented with IL-2 (100 U/mL) as required over 7 days. In preparation for labelling, cells were collected from culture dishes, washed with PBS, and re-suspended in cRPMI without antibiotics.

# 2) Bone Marrow Isolation and Differentiation (DCs and MDCSs)

Tibias and fibulas were isolated from mice and sterilized in 70% ethanol. Marrow was flushed out with PBS using a 25-gauge needle and syringe. Red blood cells (RBCs) were lysed with 1X RBC lysis buffer (Tonbo Biosciences) in PBS for 3 minutes. Cells were washed in PBS and re-suspended at 3 x $10^5$ cells/ mL in cRPMI with antibiotics supplemented with either GM-CSF (20 ng/mL, Peprotech) alone or with IL-6 (40 ng/mL, Peprotech) to drive differentiation of either DCs or MDSCs, respectively. Each cell type was cultured separately. Cells were cultured in 10 cm petri dishes (3 x $10^6$ cells in 10 mL of media/ dish) for 10 days. Fresh media (10 mL) with the same GM-CSF/IL-6 cytokine concentrations as day 0 was added on day 3 of culture. On day 6, 10 mL of cells were collected via gentle washing centrifuged at 300 x g for 5 minutes, resuspended in fresh media with the same cytokine concentrations as before and returned to

the dish. All cells were collected on day 10. Cell collection from DC plates was done gently to not disturb adherent cells (collected only cells in suspension), whereas MDSCs were collected using a cell scraper (collected only adherent cells). Cells were washed in PBS and re-suspended in cRPMI without antibiotics in preparation for labelling.

# Cell Labelling with SPIO and MEs

All cells were passaged into cRPMI without antibiotics at least one day prior to labelling with SPIO or MEs. For SPIO labelling, DCs and MDSCs were incubated at 2 x $10^6$ cells/mL with 0.03 mg/mL of Molday ION Rhodamine B (Biopal, Worchester, MA, US) in cRPMI without antibiotics for 21 hours. For ME labelling, MEs (Trade name Magnelles, obtained from Bell Biosystems Inc., San Francisco, CA[5]) were prepared as per supplier instructions. Briefly, frozen vials containing MEs were thawed at 37°C, transferred to a conical tube, and centrifuged at 3000 x g for 15 minutes. The supernatant was removed and MEs were re-suspended in antibiotic-free cRPMI. Cells and MEs were combined in a 12-well plate at the volumes and concentrations shown in Supplementary Table 1 and cultured for 17–30 hours. ME labelling ratios (ratio of the total number of magnetotactic bacteria to immune cells; MLRs) of either or both 1000 and 2000 were evaluated. DCs were tested at 1000 MLR, whereas CTLs and MDSCs were tested at both 1000 and 2000 MLR. Following incubation cells were washed twice in PBS and re-suspended in cRPMI with standard 100 U/mL penicillin/streptomycin to clear away extracellular bacteria.

Iron Quantification

# 1) Prussian Blue Assay for Quantification of Intracellular Iron Following SPIO Labelling

Intracellular iron in cells labelled with SPIO was quantified using a colorimetric Prussian Blue assay. A sample of 1–2 million cells was first lysed in 100 µL of 1M hydrochloric acid (HCL, MilliporeSigma) overnight at 37°C. The sample was centrifuged at 300 x g for 5 minutes and the supernatant was transferred to a fresh tube. One hundred microlitres of 1N potassium ferrocyanate ($K_4Fe(CN)_6$, Alfa Aesar, Ward Hill, MA, US) was then added to the sample, resulting in blue colour in the presence of iron. Absorbance was measured using ultraviolet/visible light spectrophotometry (l = 620 nm). Quantification was achieved by comparison to a standard curve of known iron concentrations ranging from 0.01 to 0.1 mg/ml. Iron per cell was derived by dividing total iron by the number of cells in the sample.

# 2) Ferrozine Assay for Quantification of Intracellular Iron Following ME Labelling

Intracellular iron in cells labelled with MEs was quantified using a specialized colorimetric Ferrozine assay (Bell Biosystems Inc.) as per supplier instructions. Briefly, 5 x $10^5$ cells were lysed by heating the sample to 75°C in 1.5M HCL for 2 hours. The sample was centrifuged at 300 x g for 5 min and supernatant was transferred to a new tube. The Ferrozine iron probe was added to the sample, producing

purple colour in the presence of iron. Absorbance was measured using ultraviolet/visible light spectrophotometry (l = 570 nm).

# Cell Phenotyping with Flow Cytometry

Cell surface markers of cultured CTLs, MDSCs, and DCs were assessed using immunocytochemistry (ICC) and flow cytometry. ICC labelling was performed by first washing samples of 2–3 million cells three times in cold PBS. Following the third wash, cells were resuspended in 50 µL of PBS with 1 µL of Fc block (eBioscience, San Diego, CA, US) and incubated at room temperature for 10 minutes. Following Fc blocking, 50 µL of PBS containing pre-conjugated antibody (Ab) was added to the tube and the sample was incubated for 30 minutes at 4°C. Following Ab incubation, cells were washed three times in cold PBS and resuspended in 300 µL of 4% paraformaldehyde (PFA; MilliporeSigma) in PBS for 10 minutes. Cells were then washed and resuspended in PBS and either immediately analyzed by flow cytometry or kept at 4°C until analysis.

# In Vitro Characterization of ME Immune Cell Labelling

# Preparation of MDSC Cell Standards for In Vitro MRI

ME-labelled MDSCs, SPIO-labelled MDSCs, and unlabelled MDSCs were prepared at increasing concentrations (0.5, 1, 1.5, and 2 x $10^6$ cells for each type) in a small volume of PBS (100 µL) and then suspended in 2 mL of warm 8% Knox gelatine (ED Smith Foods, Winona, ON, CA). The gelatine-cell mixtures were quickly transferred to 5 mm NMR tubes and set on ice until imaging.

# In Vitro MRI

Data was acquired on a 3T preclinical magnet. The magnet was equipped with a 21-cm i.d. gradient coil (200 mT/m; Magnex Scientific, Oxford, UK) interfaced with a Varian DD Console (Varian Inc., Palo Alto, California, USA). A 30 mm i.d. quadrature transmit/receive RF coil (Doty Scientific, Columbia, South Carolina, USA) was used for acquisition. $T_2$* values were obtained by measuring the linewidth of individual samples with a non-spatially resolved hard pulse and using the relation $R_2$* = π * linewidth. $T_2$* was calculated as 1/$R_2$*.

# MDSC Suppression Assay

T cell proliferation in the presence of MDSCs was measured to assess the presence of a suppressive phenotype. T cells were acutely isolated from LNs as previously described[10]. Following RBC lysis, the resulting isolate was used as responder T-cells (Tresps). Tresps were washed twice in PBS to remove any FBS and then resuspended in PBS at 1 x $10^7$ cells/ mL. Cells were combined 1:1 with a warm 1 mM solution of e670 proliferation dye (eBioscience) in PBS and incubated for 10 minutes in the dark at 37°C. Labelling was halted by adding 4–5 volumes of cold cRPMI and incubating on ice for 5 minutes. Cells were washed three times and resuspended at 1 x $10^6$ cells/ mL in cRPMI. MDSCs – either naïve, SPIO-labelled, or ME-labelled – were collected, washed, resuspended at 1 x $10^7$ cells/ mL.in cRPMI, and stored

on ice until ready to use. Cells were combined in a round-bottom 96-well plate in the amounts shown in Supplementary Table 2. All samples were plated in triplicate or more, avoiding outer wells. Outer wells were filled with water to reduce evaporation. Anti-CD3/ Anti-CD28 coated dynabeads (Gibco) were added to appropriate wells to activate Tresps. Following 72 hours in culture, samples were pooled, labelled by anti-TCRb-PerCP-Cy5.5 (clone H57-597, Invitrogen, Waltham, MA, US) and anti-CD4-PE (clone GK1.5, eBioscience), and analyzed for e670 peak distribution (more peaks indicates proliferation) by flow cytometry to demonstrate suppression (or lack thereof) of Tresps.

# Immunocytochemical Labelling

Cells were fixed by resuspending in 4% PFA in PBS for 10 minutes at room temperature and were then washed twice in PBS. Cells were permeabilized by incubating in 0.1% Triton-X (MilliporeSigma) with 1% bovine serum albumin (BSA; MilliporeSigma) in PBS for 3 minutes at room temperature, washed twice in PBS, and incubated in Alexa 488 phalloidin (Invitrogen) for 20 minutes at room temperature ($2 \times 10^6$ cells in 200 mL of PBS with 5 mL of 6 mM Alexa 488 phalloidin stock solution). Cells were then washed twice in PBS. ME-labelled cells were further labelled with rabbit anti-ME 594 (Bell Biosystems Inc., 1:1000 in 1% BSA in PBS) for 1 hour at room temperature and then washed twice in PBS. After labelling was complete, cells were resuspended in 8 µL of Fluoromount G with DAPI (eBioscience), transferred to a slide, coverslipped and sealed with clear nail polish.

# Confocal Imaging

Slides were imaged using a Zeiss LSM 710 laser scanning confocal microscope (Carl Zeiss SBE, LLC, Thornwood, New York, USA) equipped with an XBO 50Wlamp for 4',6-diamidino-2-phenylindole fluorescence (lex365, lem420 nm), an Argon laser (lex488 nm) with a 515 to 565 band-pass filter, and a HeNe laser for 548 and 633 nm excitation with a low-pass filter at 590 nm. Z-stacks were acquired for all images with a step size of 1 µm and upper and lower limits set to ensure all cells in the field of view were captured in-focus. Imaging parameters were set to include two averages per pixel at 1 A.U., a pixel dwell time of 6 msec, and 1024 x 1024 resolution.

# In Vivo Tracking of ME-Labelled MDSCs

# MDSC culture and labelling

Six days prior to cell injections, femurs and tibias were harvested from disease-matched donor mice. Bone marrow was flushed from femurs and tibias with a 25-gauge needle using PBS and RBCs were lysed with 1X RBC lysis buffer. The remaining cells were cultured for 5 days in cRPMI supplemented with GM-CSF (20 ng/mL) and IL-6 (40 ng/mL); see *in vitro* methods for further details on cell isolation and culture. Penicillin/streptomycin was omitted in media intended for use with MEs or ME-labelled cells. MDSCs were then incubated at a concentration of $2 \times 10^6$ cells/mL with either 0.03 mg/mL SPIO-Rhodamine B for 21 hours or with MEs at an MLR of 1000 for 16 hours.

# MDSC injections

MDSCs, labelled with either SPIO-Rhodamine B or MEs, were washed and resuspended in HBSS with 20 mM HEPES buffer at 15 x $10^6$ cells/mL. Recipient mice were injected with 3 x $10^6$ MDSCs (SPIO-labelled MDSCs, n = 8; ME-labelled MDSCs, n = 5) via tail vein at 23 days post-C3 implant. The remaining cells were used to quantify iron loading using the same assays as for *in vitro* studies.

# Termination and tissue collection

One mouse from each group was terminated on days 24, 26, and 28 post-C3 implant for tissue collection. Remaining mice were terminated following the last day of imaging (8 days post cell injection). Spleens, tumours, and inguinal lymph nodes were harvested and either processed for flow cytometry or flash frozen in a 2:1 mixture of optimal cutting temperature compound (OCT; Fisher Healthcare, Houston, TX, US) and 20% sucrose in PBS for immunohistochemistry.

# Immunohistochemistry of frozen tissues

Cryosectioning of tumours was performed by the Pathology Department at the IWK Health Centre (Halifax, N.S., Canada). Slides were fixed with 200 µL of 4% PFA for 15 minutes and then permeabilized with 200 µL of 0.5% Triton-X in PBS for 15 minutes. Samples were washed with PBS and blocked in 150 µL of 2% BSA in PBS for 1 hour at room temperature. Samples were washed twice with PBS and incubated with the appropriate antibodies. Tissues of mice injected SPIO-labelled MDSC injections were incubated with anti-Gr-1 eFluor 660 (1:250; clone RBC-8C5, eBioscience) in 1% BSA in PBS overnight at 4°C. Tissues were washed three times with PBS and mounted with Fluoromount-G with DAPI. Tissue slides from mice injected with ME-labelled MDSCs were incubated with rabbit anti-ME (Bell Biosystems Inc.) antibody diluted 1:1000 in PBS and anti-Gr-1 eFluor 660 (1:250; clone RBC-8C5) in 1% BSA in PBS overnight at 4°C. Slides were washed three times with PBS and then incubated with goat anti-rabbit Alexa 594 (2 drops/mL PBS IgG H + L Ready Probes™, Invitrogen) for 1 hour at room temperature. Slides were washed again three times with PBS and mounted with Fluoromount G with DAPI. Confocal imaging was done using the same microscope used for *in vitro* studies.

# MRI Acquisition

The MRI and RF coil used for *in vitro* studies was used to image tumours and inguinal lymph nodes. Mice were anesthetized using ~ 2% isofluorane during MRI scans. Anatomical images were obtained using a 3D balanced steady-state free precession[28,29] sequence (repetition time (TR)/echo time (TE) = 8/4 ms, flip angle = 30 °, 38.4 × 25.5 × 25.5 mm field of view (FOV), 256 × 170 × 170 matrix centered on the torso, 200 µm isotropic resolution). Measurements from injected MDSCs was determined using $R_2$* maps acquired using the multi-echo single point imaging sequence, TurboSPI[9,30,31]: TR = 250.0 ms, ETL = 8.0 ms, ESP = 10.0 ms, 90° flip angle, FOV of 25 x 25 x 25 mm, 96 x 96 x 48 matrix, 8x acceleration factor. The in-plane resolution was 320 µm with 0.5 mm slices. A Fast Spin Echo (FSE) image was acquired immediately before TurboSPI as a reference for TurboSPI image reconstruction. Total scan time per mouse was approximately 2 hours. Following injections with either SPIO-labelled or ME-labelled MDSCs on day 23 post-C3 implant, imaging occurred on days 24, 25, 26, 27, 28, and 31 post-implant.

# MRI Image Analysis

All images (anatomical, FSE, and $R_2$* maps) were converted into NiFTI files and imported into Vivoquant (InVicro, Boston, MA, USA). Regions of interest (ROIs; tumours and inguinal lymph nodes) were hand-drawn in VivoQuant and verified by a reviewer. The tumour and lymph node ROIs encompassed the entire tissue structure. MDSC recruitment was quantified by extracting frequency histograms of the $R_2$* values within each 3D ROI. The histograms were converted from $R_2$* values per voxel to cells per $mm^3$ using the calibration curves for SPIO-labelled MDSCs and ME-labelled MDSCs. All voxels in the ROI were summed.

# Statistical Analysis

Analyses were done using GraphPad Prism 8 (San Diego, CA, USA). Linear regression was done to generate a line of best fit for $R_2$* vs cellular concentration. A one-way ANOVA and student t-tests were used to evaluate whether there were any significant differences between ME-labelled MDSCs and SPIO-labelled MDSCs.

## RESULTS

# In Vitro Characterization of ME-Labelled Cells

We labelled three different cell types with MEs using two potential loading ratios (MLRs) and evaluated iron (Fe) loading per cell (see Table 1). Increasing the MLR had a significant effect on Fe loading in MDSCs, causing a more than 3-fold increase in pg/cell when going from an MLR of 1000 to 2000. The Fe loading achieved with 2000 MLR was comparable to what was achieved with SPIO. However, for CD8 cells, doubling MLR and increasing loading time did not increase Fe loading past 0.3 pg/cell, which is only a tenth of that seen in SPIO. For DCs, an MLR of 1000 led to a loading of 1.4 pg Fe per cell – significantly less than that achieved with SPIO. Fe loading of DCs at an MLR of 2000 was unable to be assessed due to sample volume limitations.

Table 1
Iron Labeling Results for Immune Cells

| | SPIO | | ME | | |
|---|---|---|---|---|---|
| | **Duration (hours)** | **Fe Loading (pg per cell)** | **MLR** | **Duration (hours)** | **Fe Loading (pg per cell)** |
| **MDSC** | 17 | 1.9 | 1000 | 17 | 0.63 |
| | N/A | | 2000 | 22 | 2.22 |
| **CD8** | 22 | 3.0 | 1000 | 21 | 0.22 |
| | N/A | | 2000 | 30 | 0.30 |
| **DC** | 17 | 9.8 | 1000 | 17 | 1.40 |

ICC of ME-labelled cells demonstrated that MEs were present and localized within cells (Figs. 1 and 2). Clusters of MEs were visible inside DCs at MLRs of 1000 and 2000 (Fig. 1), and SPIO is also readily visible inside cells. MEs were also readily visible inside MDSCs (Fig. 2).

The MDSC suppression assay (Fig. 2B), demonstrated that MDSCs labelled with either SPIO (3rd column) or MEs using an MLR of 1000 (2nd column) retained comparable suppressive ability to unlabelled MDSCs, even at a wide range of Tresp:MDSC ratios. However, MDSCs labelled at an MLR of 2000 had reduced suppressive capacity, with T cell proliferation observed with all Treps:MDSC ratios.

Further characterization of ME-labelled cells focused on MDSCs with an MLR of 1000 due to their strong labelling as well as high purity and robustness in culture. The magnetic characteristics/contrast of SPIO- and ME-labelled MDSCs were evaluated using *in vitro* labelled MDSCs in tubes (Fig. 3). The $R_2$* was plotted against cellular concentration in the tubes, and linear regression was done in Prism to generate a line of best fit. There was a significant non-zero slope (** indicates $p < 0.05$) for both SPIO-labelled MDSCs and ME-labelled MDSCs. SPIO-labelled MDSCs demonstrated a higher slope than ME-labelled MDSCs (0.03482$mm^3$/cells*s vs 0.01859 $mm^3$/cells*s), which is consistent with the higher Fe loading observed in SPIO-labelled MDSCs as measured in our iron assays.

# In Vivo Tracking of ME-Labelled MDSCs

MDSCs were isolated from the bone marrow of tumour-bearing mice approximately 21 days post-C3 implant and cultured *in vitro* for 7 days (6 days for growth, last day for iron labelling). A subset of MDSCs was phenotyped using flow cytometry (Supplementary Fig. 2) prior to labelling with iron due to the potential for the Rhodamine tag on SPIO to interfere with FACS labels. MDSCs were 100% CD11b + and were a mix of $Ly6c^{int}$/$Ly6g^{int}$ and $Ly6c^{hi}$/$Ly6g^{lo}$, suggesting the presence of MDSC subpopulations.

Cultured MDSCs were labelled with either SPIO or MEs and then injected i.v. into tumour-bearing mice approximately 23 days post-implant. Mice were imaged 24, 48, 72, 96, 120 and 192 hours post-injection. Representative anatomical MR images with the $R_2$* map overlaid are shown in Fig. 4 for both label types and three time points. Both labelled cell types were present in tumours for up to 8 days post-injection. Labelled MDSCs are more densely recruited to the periphery of tumours, which is similar to what is seen in previous studies[10]. Recruitment patterns were comparable between SPIO-labelled MDSCs and ME-labelled MDSCs.

Turbo SPI maps were used to quantify cell recruitment based on known iron uptake in each cell type. The number of SPIO-labelled MDSCs was stable over the 8-day period (Fig. 5a), which is consistent with SPIO degradation rates seen anecdotally in our lab and in previous studies[9,10]. Interestingly, the number of ME-labelled MDSCs was also stable over time and consistently higher than the number of SPIO-labelled MDSCs present. While the number of ME- vs. SPIO-labelled cells was not significantly different on any given day, overall, using a mixed-model analysis, the cell label had a significant effect ($p = 0.0042$) on the

number of recruited cells over the whole data set. ME-labelled MDSC numbers were more variable between mice than those of SPIO-labelled MDSCs, particularly at the latest time points.

To confirm labelled cells on MR images were, in fact, MDSCs, tumours were removed, sectioned, and analysed with IHC. Both SPIO and ME-labelled cells were found to be co-localized with the Gr-1 (a composite of Ly6c/Ly6g antigens; Fig. 5b).

# DISCUSSION

The use of MRI cell tracking for longitudinal studies remains limited by the eventual degradation of the primary contrast agents, typically superparamagnetic iron oxide. The objective of this study was to assess the use of MEs as a potential contrast agent for MR imaging of immune cells. MEs have previously been studied in both cancer and stem cells[22,26,32], and isolated magnetosomes have been used for labelling DCs. However, to the best of our knowledge, no one has used MEs to directly label immune cells. Given that tracking of immune-based cell therapies are one of the primary goals for many MRI labs, it is important to assess the effects that MEs have on immune cells.

Immune cells differ from other cells, and between their own subtypes, in morphology and function, which can result in variable uptake of contrast agents. Therefore, this project began with three different immune cell types and two different ME loading ratios (MLRs) at the *in vitro* level, before choosing the most promising cell type and conditions to progress to *in vivo* experiments.

The smallest immune cells (5–7μm), CD8 + T cells, which also have lower phagocytic activity, had much lower iron loading when labelled with MEs (0.22-0.3pg/cell, both MLRs) compared to SPIO (3pg). These results correspond well with other literature indicating average cell loading of 3-5pg iron/cell when using SPIO[9,30]. This level of iron loading in the MEs is typically on the low end of detectability in MRI cell tracking (ideally > 0.5pg/cell) indicating that MEs may not be an optimal choice for this cell type, or that if they are used, more invasive methods of labelling may be necessary, such as transporation and transfection agents.

Both MDSCs and DCs were found to have much better loading from MEs, with MDSCs ranging from 0.63-2.2pg iron/cell and DCs having approximately 1.7pg/cell. Notably, MDSCs, a normally suppressive cell type, demonstrated impaired suppression of T cell growth when labelled with a higher number of MEs (2000MLR). This may be due to pathogen-associated molecular pattern (PAMP) signaling induced by the MEs (which are bacterial) which can cause differentiation and/or maturation of MDSCs and DCs[33–35]. Due to observed dysfunction at the higher MLR, it was decided to use an MLR of 1000 for the remaining experiments. Although both MDSCs and DCs had acceptable iron labelling (considered at a minimum, > 0.5 pg/cell), only the MDSCs were used for this *in vivo* study. Future studies will explore other cell types.

Previous studies using cardiomyocytes (approximately100-150 μm x 20–25 μm in dimension), neural stem cells (< 12 μm diameter), and cancer cells (15–25 μm in diameter) indicated that it was possible to use much higher MLRs for these cell types[5,22,26,32]. Given the range of sizes of these cells, it may not be

purely a case of larger cells being able to hold more MEs. Also, when present in larger numbers, MEs may impact function in some cell types, while minimally affecting others. Therefore, any studies looking to use MEs should perform *in vitro* cell-type-specific characterizations of cellular function with different MLRs before proceeding to *in vivo* studies.

It is important to note that this study does not assess the longevity of the MEs themselves. Due to the tumor model used, we were limited to an 8–10 day observation period before humane endpoint issues from tumor growth could occur. It is known from recent work[26] that, if unmodified, MEs will eventually end up in the phagocytic pathway of cell digestion. Research to modify the ME coating to eliminate or delay these phagocytic effects is ongoing by other groups[26] but is outside of the scope of this work. Interestingly, previous work has demonstrated that even when MEs themselves are undergoing degradation, the magnetosomes remain intact in live cells for considerably longer, with Lee et al[26] demonstrating their presence in cancer cells at least 48 hours post-injection (no data was acquired past that point) and McGinley et al[32] demonstrating MR contrast in tissue 14–28 days post-injection, indicating the presence of iron crystals, if not intact magnetosomes. Given the MEs in this project are unmodified, it is possible that the MEs were undergoing degradation throughout the course of the *in vivo* study, but that the magnetosomes remained intact, resulting in the MR contrast.

For *in vivo* studies, both ME- and SPIO-labeled MDSCs were detectable using TurboSPI. Both labelled cell types were generally clustered around the periphery of the tumor, which is common for immune cells in excluded tumor environments (as seen previously in this model [9,36]). $R_2$* values post-cell injection were very similar for both tumors, but given the differences in loading between the two cell types, this resulted in large differences (although not significant) between SPIO- and ME-labelled cells. At all time points, our method calculated higher cellular densities for ME-labelled cells compared to SPIO-labelled cells. This may be due to either biological effects or changes in the magnetic properties of cells. If the presence of MEs in MDSCs affected immune signalling in a way that we did not account for (our assessment was limited to suppression of T cells), it is possible that this could result in altered signalling/recruitment for other MDSCs and/or immune cells in the tumor microenviroment. There could also be changes in the amount or structure of iron, particularly over time, that we are not accounting for in our quantitative analysis. Our quantification relies on assumptions of iron in cells measured *in vitro*, but it is not clear how this may change *in vivo*. Accurate quantification of iron via biological methods is difficult with the small cell numbers present in the tumors. We are currently working on studies attempting to better validate iron content in cells *in vivo* using other tumor models and inductively coupled plasma optical emission spectroscopy.

# CONCLUSIONS

Overall, this work demonstrates that MEs can be used as a label for MRI cell tracking of immune cells, but there are many caveats that should be considered prior to their use. Given the lower iron per cell and the potential to affect cellular function, the use of MEs is not likely to be preferential compared to traditional

cell tracking agents such as SPIO over time frames such as those explored in this work. However, should researchers be able to modify MEs to improve longevity *in vivo*, then MEs could have interesting potential for future use in MRI cell tracking.

# Declarations


### ACKNOWLEDGEMENTS

KB would like to acknowledge funding from an IWK Health Centre Project Grant and a National Science and Engineering Council (NSERC) Discovery Grant. AN was supported by an IWK postdoctoral fellowship.


### CONFLICT OF INTEREST STATEMENT

KB would like to disclose that they had a research collaboration with Bell Biosystems in the past, although it was completed prior to carrying out the work described in this manuscript.

# References


1. Dudley, M. E. & Rosenberg, S. A. Adoptive-cell-transfer therapy for the treatment of patients with cancer. *Nat Rev Cancer* **3**, 666–675 (2003).
2. Hinrichs, C. S. & Rosenberg, S. A. Exploiting the curative potential of adoptive T-cell therapy for cancer. *Immunol Rev* **257**, 56–71 (2014).
3. Vries, I. J. M. de *et al.* Magnetic resonance tracking of dendritic cells in melanoma patients for monitoring of cellular therapy. *Nat Biotechnol* **23**, 1407–1413 (2005).
4. Kumar, M., Medarova, Z., Pantazopoulos, P., Dai, G. & Moore, A. Novel membrane-permeable contrast agent for brain tumor detection by MRI. *Magnet Reson Med* **63**, 617–624 (2010).
5. Brewer, K. D. *et al.* Characterization of Magneto-Endosymbionts as MRI Cell Labeling and Tracking Agents. *Mol Imaging Biol* **3**, 595 (2017).
6. Hong, H., Yang, Y., Zhang, Y. & Cai, W. Non-invasive cell tracking in cancer and cancer therapy. *Curr Top Med Chem* **10**, 1237–48 (2009).
7. Heyn, C. *et al.* In vivo magnetic resonance imaging of single cells in mouse brain with optical validation. *Magnet Reson Med* **55**, 23–29 (2006).
8. Bulte, J. W. M. & Daldrup-Link, H. E. Clinical Tracking of Cell Transfer and Cell Transplantation: Trials and Tribulations. *Radiology* **289**, 604–615 (2018).
9. Tremblay, M.-L. *et al.* Quantitative MRI cell tracking of immune cell recruitment to tumors and draining lymph nodes in response to anti-PD-1 and a DPX-based immunotherapy. *Oncoimmunology* **9**, 1851539 (2020).
10. Tremblay, M. *et al.* Using MRI cell tracking to monitor immune cell recruitment in response to a peptide-based cancer vaccine. *Magnet Reson Med* **80**, 304–316 (2018).

11. Zhang, X. *et al.* Cellular magnetic resonance imaging of monocyte-derived dendritic cell migration from healthy donors and cancer patients as assessed in a scid mouse model. *Cytotherapy* **13**, 1234–1248 (2011).
12. Chickera, S. de *et al.* Cellular MRI as a suitable, sensitive non-invasive modality for correlating in vivo migratory efficiencies of different dendritic cell populations with subsequent immunological outcomes. *Int. Immunol.* **24**, 29–41 (2012).
13. Tavaré, R. *et al.* Monitoring of In Vivo Function of Superparamagnetic Iron Oxide Labelled Murine Dendritic Cells during Anti-Tumour Vaccination. *PLoS ONE* **6**, e19662-11 (2011).
14. Brewer, K. D. *et al.* Clearance of depot vaccine SPIO-labeled antigen and substrate visualized using MRI. *Vaccine* **32**, 6956–6962 (2014).
15. Schoepf, U., Marecos, E. M., Melder, R. J., Jain, R. K. & Weissleder, R. Intracellular Magnetic Labeling of Lymphocytes for In Vivo Trafficking Studies. *Biotechniques* **24**, 642–651 (1998).
16. Frank, J. A. *et al.* Clinically applicable labeling of mammalian and stem cells by combining superparamagnetic iron oxides and transfection agents. *Radiology* **228**, 480–7 (2003).
17. Rad, A. M., Janic, B., Iskander, A., Soltanian-Zadeh, H. & Arbab, A. S. Measurement of quantity of iron in magnetically labeled cells: comparison among different UV/VIS spectrometric methods. *Biotechniques* **43**, 627–636 (2007).
18. Heyn, C., Bowen, C. V., Rutt, B. K. & Foster, P. J. Detection threshold of single SPIO-labeled cells with FIESTA. *Magn Reson Med* **53**, 312–320 (2005).
19. Pawelczyk, E. *et al.* In Vivo Transfer of Intracellular Labels from Locally Implanted Bone Marrow Stromal Cells to Resident Tissue Macrophages. *Plos One* **4**, e6712 (2009).
20. Alphandéry, E. Applications of Magnetosomes Synthesized by Magnetotactic Bacteria in Medicine. *Frontiers Bioeng Biotechnology* **2**, 5 (2014).
21. Mériaux, S. *et al.* Magnetosomes, Biogenic Magnetic Nanomaterials for Brain Molecular Imaging with 17.2 T MRI Scanner. *Adv Healthc Mater* **4**, 1076–1083 (2015).
22. Mahmoudi, M. *et al.* Novel MRI Contrast Agent from Magnetotactic Bacteria Enables In Vivo Tracking of iPSC-derived Cardiomyocytes. *Sci Rep* **6**, 26960 (2016).
23. Schwarz, S. *et al.* Synthetic and biogenic magnetite nanoparticles for tracking of stem cells and dendritic cells. *J Magn Magn Mater* **321**, 1533–1538 (2009).
24. Cypriano, J. *et al.* Uptake and persistence of bacterial magnetite magnetosomes in a mammalian cell line: Implications for medical and biotechnological applications. *Plos One* **14**, e0215657 (2019).
25. Shin, J., Yoo, C.-H., Lee, J. & Cha, M. Cell response induced by internalized bacterial magnetic nanoparticles under an external static magnetic field. *Biomaterials* **33**, 5650–5657 (2012).
26. Lee, K. R. *et al.* Cell Labeling with Magneto-Endosymbionts and the Dissection of the Subcellular Location, Fate, and Host Cell Interactions. *Mol Imaging Biol* **20**, 55–64 (2018).
27. Daftarian, P. *et al.* Eradication of established HPV 16-expressing tumors by a single administration of a vaccine composed of a liposome-encapsulated CTL-T helper fusion peptide in a water-in-oil

emulsion. *Vaccine* **24**, 5235–5244 (2006).

28. Scheffler, K. On the transient phase of balanced SSFP sequences. *Magn Reson Med* **49**, 781–783 (2003).
29. Scheffler, K. & Lehnhardt, S. Principles and applications of balanced SSFP techniques. *Eur Radiol* **13**, 2409–2418 (2003).
30. O'Brien-Moran, Z., Bowen, C. V., Rioux, J. A. & Brewer, K. D. Cell density quantification with TurboSPI: R2* mapping with compensation for off-resonance fat modulation. *MAGMA* **3**, 250–13 (2019).
31. Rioux, J. A., Brewer, K. D., Beyea, S. D. & Bowen, C. V. Quantification of superparamagnetic iron oxide with large dynamic range using TurboSPI. *J. Magn. Reson.* **216**, 152–160 (2012).
32. McGinley, L. M. *et al.* Magnetic resonance imaging of human neural stem cells in rodent and primate brain. *Stem Cell Transl Med* **10**, 83–97 (2020).
33. Ost, M. *et al.* Myeloid-Derived Suppressor Cells in Bacterial Infections. *Front Cell Infect Mi* **6**, 37 (2016).
34. Nelson, N. L. J., Zajd, C. M., Lennartz, M. R. & Gosselin, E. J. Fcγ receptors and toll-like receptor 9 synergize to drive immune complex-induced dendritic cell maturation. *Cell Immunol* **345**, 103962 (2019).
35. Sepulveda-Toepfer, J. A. *et al.* TLR9-mediated activation of dendritic cells by CD32 targeting for the generation of highly immunostimulatory vaccines. *Hum Vacc Immunother* **15**, 179–188 (2019).
36. Tremblay, M.-L. *et al.* Abstract 384: T cell infiltration into tumors induced by DPX-Survivac combination immunotherapy demonstrated by PET/MRI imaging in an orthotopic ovarian cancer model. *Cancer Res.* **80**, 384–384 (2020).

# Figures

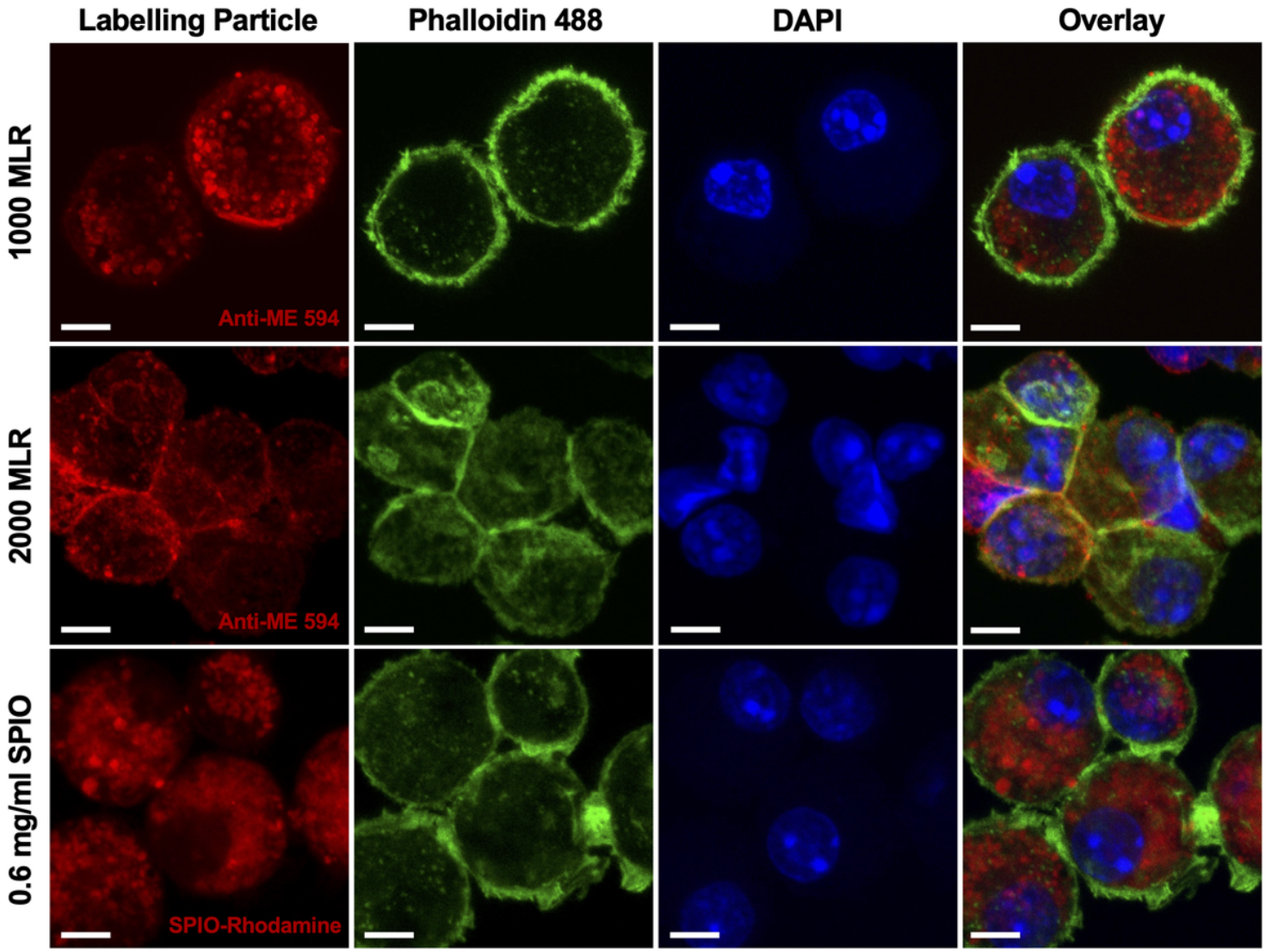


## Figure 1

ME and SPIO Labeling of BM-DCs. Top row: ME-labeling of BM-DCs after 20-hour incubation at 1000 MLR. Middle row: ME-labeling of BM-DCs after 20-hour incubation at 2000 MLR. Labels for top and middle rows: anti-ME (red); phalloidin (green); DAPI (blue). Bottom row: SPIO-labeling of BM-DCs after a 20-hour incubation with 0.6 mg/mL SPIO in media. Labels for bottom row: SPIO-Rhodamine (red), phalloidin (green), DAPI (blue). Note that phalloidin stains cell walls, while DAPI is a nuclear stain. All scales are 5 mm.

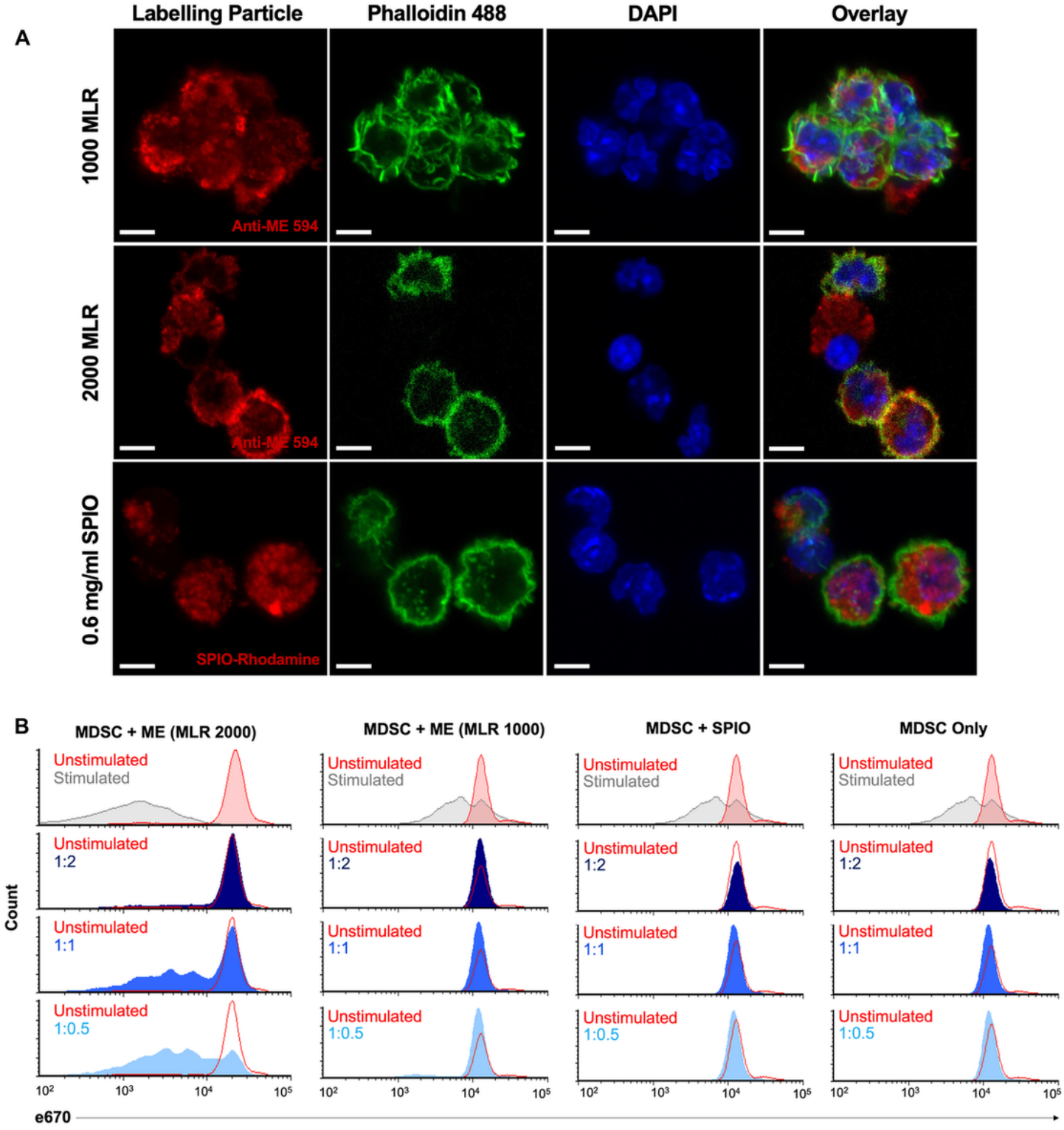


## Figure 2

ME and SPIO Labeling of BM-MDSCs and Suppression Assay. A) IHC - Top row: ME-labeling of BM-MDSCs after 20-hour incubation at 1000 MLR. Middle row: ME-labeling of BM-MDSCs after 20-hour incubation at 2000 MLR. Labels (top and middle rows): anti-ME (red); phalloidin (green); DAPI (blue).Bottom row: SPIO-labeling of BM-MDSCs after a 20-hour incubation with 0.6 mg/mL SPIO in media. Labels (bottom row): SPIO-Rhodamine (red), phalloidin (green), DAPI (blue). All scales are 5 mm.

B) MDSC Suppression Assay. Unstimulated T cells are shown in red and stimulated T cells in grey. Blue traces show stimulated T cells co-incubated with varying ratios of MDSCs (Tresp:MDSC). MDSC suppression of T cells was unaffected by MLR 1000 and SPIO labelling (middle columns) but was impaired in the MLR 2000 condition (first column), as shown by the appearance of lower intensity peaks caused by dilution of the e670 dye in T cells during proliferation. Tresps and MDSCs were gated for singlets and viability (zombie dye). Tresps were further gated as CD4+ T cells only.

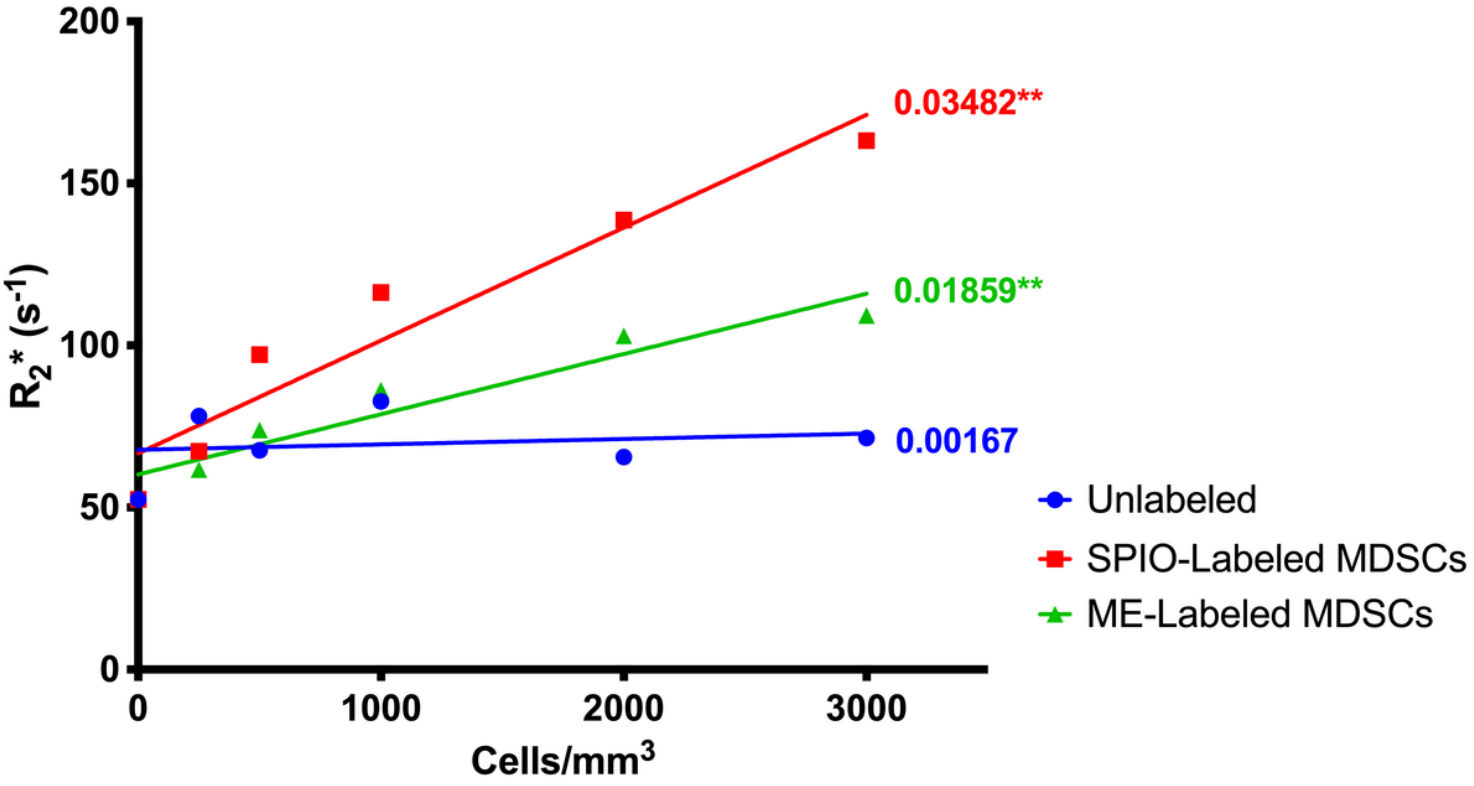


**Figure 3**

*In Vitro* $R_2$* characterization of ME and SPIO-labeled MDSCs. For both labeled and unlabeled cells, 0.5, 1, 1.5, and 2 x $10^6$ cells were prepared in 2mL gelatin in 5mm NMR tubes. Bulk $R_2$* measurement was done across the whole tube and $R_2$* values were plotted against the cellular concentration. A line of best fit was generated using the linear regression package in GraphPad Prism; the slopes of these fits are given next to the lines. ** indicates the slope was significantly non-zero with $p<0.05$. For both labeled MDSC types, the lines of best fits had $R^2>0.9$.

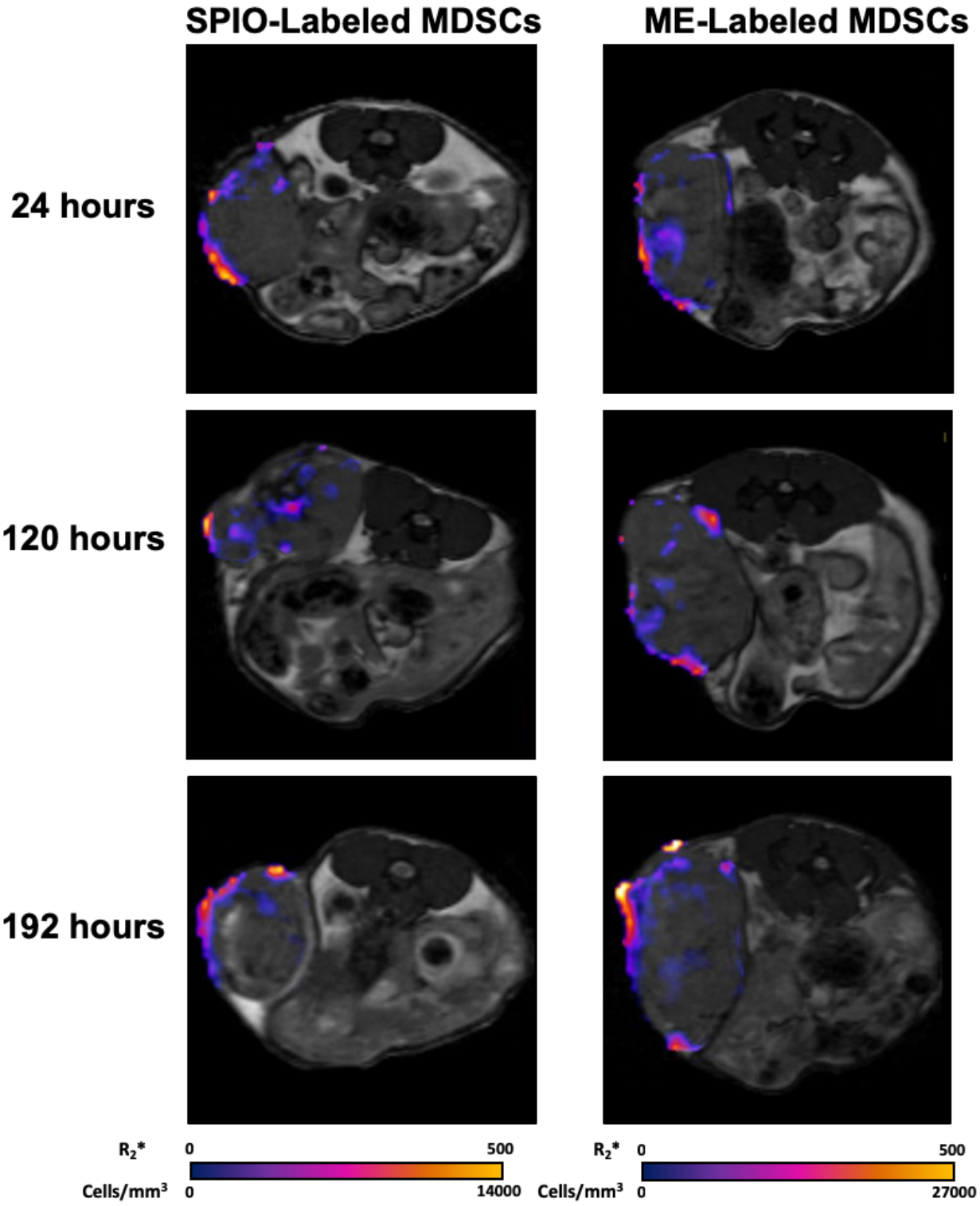


## Figure 4

Representative *in vivo* MR images of SPIO and ME-labeled MDSCs in a murine cervical cancer model. The anatomical underlay (grey) is the bSSFP high-resolution image, and the color overlay is the TurboSPI $R_2$* map. The color bar indicates the conversion of $R_2$* to cells/mm$^3$ for each labelled cell type.

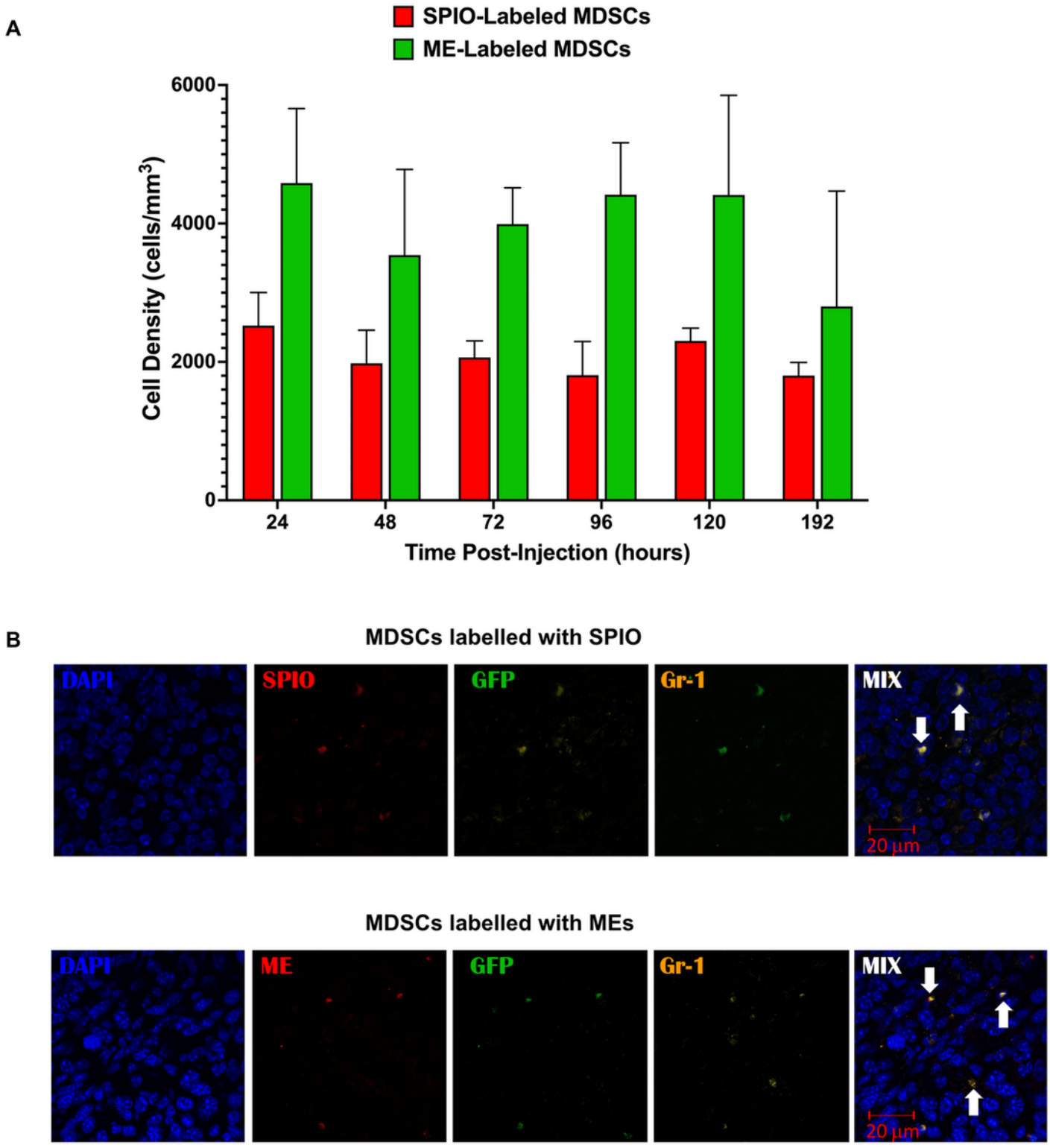


## Figure 5

*In Vivo*results of cell tracking of labeled MDSCs using MRI and IHC. A) Quantitative results of cell densities in tumours as measured by TurboSPI. Error bars represent standard error. A mixed model ANOVA indicated that there was a significant effect due to the label used (p=0.0042), however none of the individual days had significant differences due to labelling. B) IHC results from tumour tissue taken post the 120 hour timepoint. Donor cells were GFP+ (green) and were labeled with Gr-1 (far red) and DAPI

(blue). SPIO was conjugated to rhodamine (red), and MEs were labelled with Alexa 594 (red). White arrows indicate positively labeled Gr-1+ donor cells. Images were acquired at 100X magnification and scale bar is shown on the rightmost panel for each label type.

## Supplementary Files

This is a list of supplementary files associated with this preprint. Click to download.

- SupplementaryFiguresfinal.docx